Research Article

Xu Zhongjie, Kong Jintao*, Cheng Rihui, Lan Yizhi, and Wang Liaoliang

LA-ICP-MS U–Pb ages of detrital zircons from Middle Jurassic sedimentary rocks in southwestern Fujian: Sedimentary provenance and its geological significance

https://doi.org/10.1515/geo-2020-0185
received August 20, 2019; accepted July 23, 2020

Abstract: In order to determine the tectonic regime change of the early Mesozoic in the South China Block, this study analyzed sedimentary rocks in the Middle Jurassic of southwestern Fujian by modal analysis of sandstones, elemental geochemical analysis of mudstones, and detrital zircons U–Pb dating. The results show that the detrital zircons in Southwestern Fujian mainly consist of Paleoproterozoic to early Mesozoic zircons in the Middle Jurassic. Within the Dongkeng profile of the Zhangping Formation, DK5 sample (lower part) showed a major age peak at ca. 1,848 Ma and two secondary age peaks at ca. 235 and 180 Ma, while DK15 sample (middle part) showed a major age peak at ca. 1,876 Ma and two secondary age peaks at ca. 233 and 190 Ma; the age compositions of these two samples' were similar. Modal analysis of sandstones indicated that sediments of Zhangping Formation might source from arc orogen and recycled orogen, and element geochemical analysis showed that source rocks of Zhangping Formation might be sedimentary rocks and granites. The Indosinian zircons were mainly derived from the Wuyi region, and the Yanshanian zircons were mainly derived from the Nanling region. The major age group changes from ca. 230 to 220 Ma of the Late Triassic – Early Jurassic to ca. 190 to 180 Ma of the Middle Jurassic in Southwestern Fujian, and main sources changed from Indosinian magmatic rocks in the Late Triassic – Early Jurassic to early Yanshanian magmatic rocks in the Middle Jurassic.

Keywords: Indosinian movement, Middle Jurassic, provenance, Southern China Block, southwestern Fujian, zircon U–Pb ages

1 Introduction

The South China Block, which is located at the connection of Paleo-Asia, Tethys, and Circum-Pacific, is divided into the Cathaysia and the Yangtze Blocks, and its geological structure is very complicated due to the special tectonic position [1,2]. During the early Mesozoic, the eastern and western South China Blocks were related to the evolution of the Paleo-Pacific and Paleo-Tethyan tectonic domains, respectively, and these regions were greatly influenced by Indosinian and Yanshanian movements [3,4]. The Indosinian and Yanshanian movements in the middle Mesozoic established the mainland tectonic configuration of South China Block and eastern China nowadays, but the relationship between these two movements and the Paleo-Tethys and Paleo-Pacific is still controversial. Some scholars believe that the Indosinian movement in South China Block is controlled by the closure of Paleo-Tethys [5–8], and other scholars have suggested that the two tectonic events are related to the subduction of the Paleo-Pacific Block beneath East Asian Block [9–12]. The Paleo-Tethys and Paleo-Pacific tectonic regimes are not only different in terms of paleontology and paleoclimate, but also mainly in terms of the tectonic nature, its geological effects, and the basin sediments compositions.

Southwestern Fujian is located in the southeastern South China Block. It is one of the land regions close to the shelf-slope region of the northern South China Sea. Southwestern Fujian region is connected with the Philippine Block across the Taiwan Strait and has an essential position in the tectonic pattern of South China

* **Corresponding author: Kong Jintao,** College of Earth Sciences, Jilin University, Changchun 130061, Jilin, China; Key Laboratory of Marine Reservoir Evolution and Hydrocarbon Accumulation Mechanism, Chinese Ministry of Education, Changchun 130061, China, e-mail: kongjt17@mails.jlu.edu.cn
Xu Zhongjie: College of Earth Sciences, Jilin University, Changchun 130061, Jilin, China; Key Laboratory of Marine Reservoir Evolution and Hydrocarbon Accumulation Mechanism, Chinese Ministry of Education, Changchun 130061, China
Cheng Rihui, Lan Yizhi: College of Earth Sciences, Jilin University, Changchun 130061, Jilin, China
Wang Liaoliang: Guangzhou Bureau of Marine Geology Survey, Guangzhou 510075, Guangdong, China

Block. The northeastern shelf-slope region of the South China Sea is the extension underwater of the South China Block geologically. Thus, there are some continuities and comparable features in terms of the development and distribution between the land and sea during the Mesozoic. The evolution of marine basins must have been affected by the tectonic background of the South China Block [13]. Studies on the sedimentary sources and basin properties of early Mesozoic basins in southwestern Fujian will be of great significance for oil-gas exploration of the Mesozoic basin in northern South China Block.

At present, there have been many useful research results in regard to southwestern Fujian's sedimentary environment, paleogeography [14–16], paleoclimate, and tectonic background [17,18]. The Middle Jurassic was an important period for the basin evolution, sea-land change, and paleogeographic pattern evolution. The sedimentary processes and sediments in the sedimentary basin must have retained important information about the tectonic process and geological events about source areas. Detrital zircons in clastic rocks have excellent stability and comprise extensive age information, so detrital zircons U–Pb dating has become an effective method for provenance research in recent years [19–25]. Wang et al. [26] used detrital zircon age information to explore the sediment compositions and changes in the Wenbishan Formation during the Late Triassic in southwestern Fujian. However, provenance studies during the Middle Jurassic in southwestern Fujian remain incomplete in which evidence is lacking in regard to sedimentary detrital zircon U–Pb ages. Besides, many scholars have proposed that major elements, trace elements and rare earth elements (REEs), in sediments can provide important information for the provenance of sediments [27–33]; especially, some trace and REEs in the mudstone are relatively stable and not affected by weathering and sedimentation, which can reflect the geochemical properties of the provenance well [27]. Therefore, this study presents comparisons of detrital zircon data for sedimentary rocks around the study area during late Paleozoic-early Mesozoic, based on modal analysis, detrital zircon isotopic ages, and element geochemical characteristics of the sedimentary rocks from the Middle Jurassic in southwestern Fujian. Our objective was to determine the sediment sources in the Middle Jurassic of southwestern Fujian and to explore the response to tectonic regime change in sedimentary strata of the early Mesozoic in South China Block.

2 Geological setting

Fujian region can be divided into five tectonic units: the Wuyi ancient arc-basin, the Nanping-Ninghua (premature) rift valley, the southwestern Fujian epicontinental sea basin, the eastern Fujian coastal magmatic arc, and Songxi-Youxi ophiolitic melange zone [34]. Southwestern Fujian is located in the Cathaysia Block, and the study area belongs to the southwestern Fujian epicontinental sea basin. The lithostratigraphic units in the Late Triassic-Neogene of Fujian can be divided into the West Fujian stratigraphic sub-area and East Fujian stratigraphic sub-area, and southwestern Fujian is located in the West Fujian stratigraphic sub-area.

The lithology as well as facies of the Jurassic strata in southwestern Fujian is complex and the thickness is large. In southwestern Fujian, the marine sediments, transition facies sediments, and continental sediments developed during the Late Triassic – Middle Jurassic. The Late Triassic sediments have typical characteristics of molasse-like deposits and of continental lacustrine deposits [26]. In the Late Triassic, a small-scale transgression occurred in southwestern Fujian (the regions of Nanjing County – Zhangping City) and a gulf lagoon facies was present [35]. The transgression of South China Block intruded from the southeast and extended to the southwest, northwest, and northeast in the early stage of the Early Jurassic. The transgression covers eastern Guangdong, middle-southern Guangdong, northern Guangdong, and parts of Fujian [36]. Southwestern Fujian was affected by the transgression and developed shallow-coastal marine deposits in the Early Jurassic. The area of marine sediments in southwestern Fujian was significantly smaller than that in the early stage of the Early Jurassic, and volcanic rocks developed extensively. The regression in Guangdong and Fujian regions began in the late stage of the Early Jurassic [18]. In the Middle Jurassic, there were only some basins among the mountains in southwestern Fujian, and the fan delta facies, the delta facies, and lacustrine sediments were developed among these basins. The seawater was completely withdrawn from Guangdong and Fujian in the Middle Jurassic [16,18]. The southeastern South China Block (southwestern Fujian – eastern Guangdong – northern Guangdong – middle Guangdong) experienced a large-scale transgression–regression cycle, and the largest transgression occurred in the Early Jurassic. The "eastern Guangdong basin" formed in the transgression not only developed sea facies and sea-land interbedded facies with a

thickness of 5,000 m, but it was also connected with the northeastern part of the South China Sea [16]. A regression also occurred in the southeastern South China Block during the late stage of the Early Jurassic. In the Middle Jurassic, eastern Guangdong was dominated by continental lake deposits and locally developed volcanic rocks. Furthermore, the climate in southwestern Fujian was hot and dry in the Middle Jurassic and there were numerous purple and red deposits in some lacustrine basins and marshes. The other regions of southern Fujian were the denuded zone. The change in the sedimentary environment of the Late Triassic-Middle Jurassic was the result of changes in the basin type and tectonic regime [17,18].

3 Sample description

Zhangping Formation samples of the Middle Jurassic were collected from the Dongkeng profile located in northeastern Zhangping city (N: 25°18′11.2″, E: 117°25′30.8″) (Figure 1c). The Zhangping Formation is in conformable contact with the underlying Lishan Formation and in unconformable contact with the overlying Yuanpan Formation. The cumulative thickness of the Zhangping Formation in the Dongkeng profile is approximately 2,900 m.

The lithology of the lower Zhangping Formation (0–750 m) is mainly mudstone, silty mudstone blended with earthy yellow fine sandstone, and

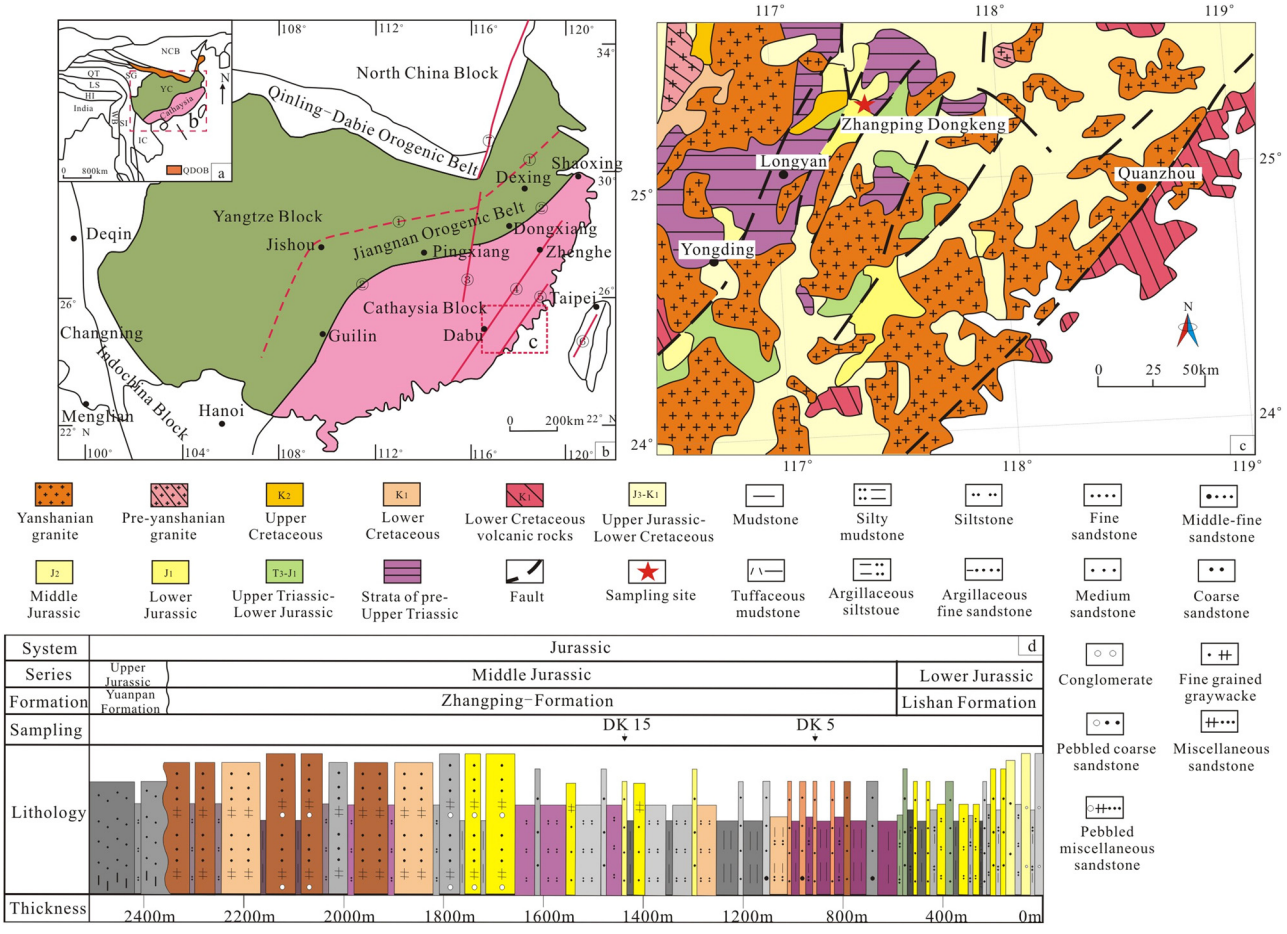

Figure 1: (a and b) Division schematic diagram of South China Block and its adjacent tectonic units (modify by Wang et al., 2013), (c) basin geological sketch in Mesozoic–Cenozoic in South China Block, (d) compiled column of Zhangping formation in Middle Jurrasic of South-West Fujian Province. YC: Yangtze Craton; QDOB: Qinling-Dabie Orogenic Belt; NCB: North China Block; IC: Indosinian Craton; SI: Sibumasu Plate; SG: Songpan-Ganzi Terrane; WB: Western Myanmar; HI: Himalaya; LS: Lhasa Block; QT: Qiangtang Terrane; (1) Jiangnan Mesozoic North Border Concealed Fault; (2) Shaoxing-Jiangshan-Pingxiang Fault Zone; (3) Ganjiang Fault Zone; (4) Zhenghe-Dabu Fault Zone; (5) Changle-Nan'ao Fault Zone; (6) Taiwan Longitudinal Valley Belt; (7) Tan-Lu Fault Zone.

medium-fine sandstone. The middle lithology is dominated by aubergine and gray-white silty sandstone blended with yellow fine sandstone. The current bedding and horizontal bedding can be observed in the mudstones layers (Figure 2a and b), and at the same time, plant fossils and ichthyolites can be observed in the silty mudstone layers (Figure 2c), lenticular bedding can be observed in the local fine sandstone layers (Figure 2d), and the erosional surface can be seen in the lower part of the fine sandstone layers (Figure 2e). The grain size of sediments in the lower Zhangping Formation is generally fine, and the lower Zhangping Formation complies with shallow lacustrine facies.

The middle Zhangping Formation, which ranges from 750 to 1,550 m, is mainly composed of aubergine, light gray and yellow siltstone with yellow medium sandstone, fine sandstone, and black gray mudstone. Siltstones and fine sandstones form reverse grain sequence deposition patterns, while wedge-shaped cross-bedding and trough cross-bedding can be observed in the fine sandstone layers (Figure 2f and g), and horizontal bedding can be observed in the mudstone layers (Figure 2h).

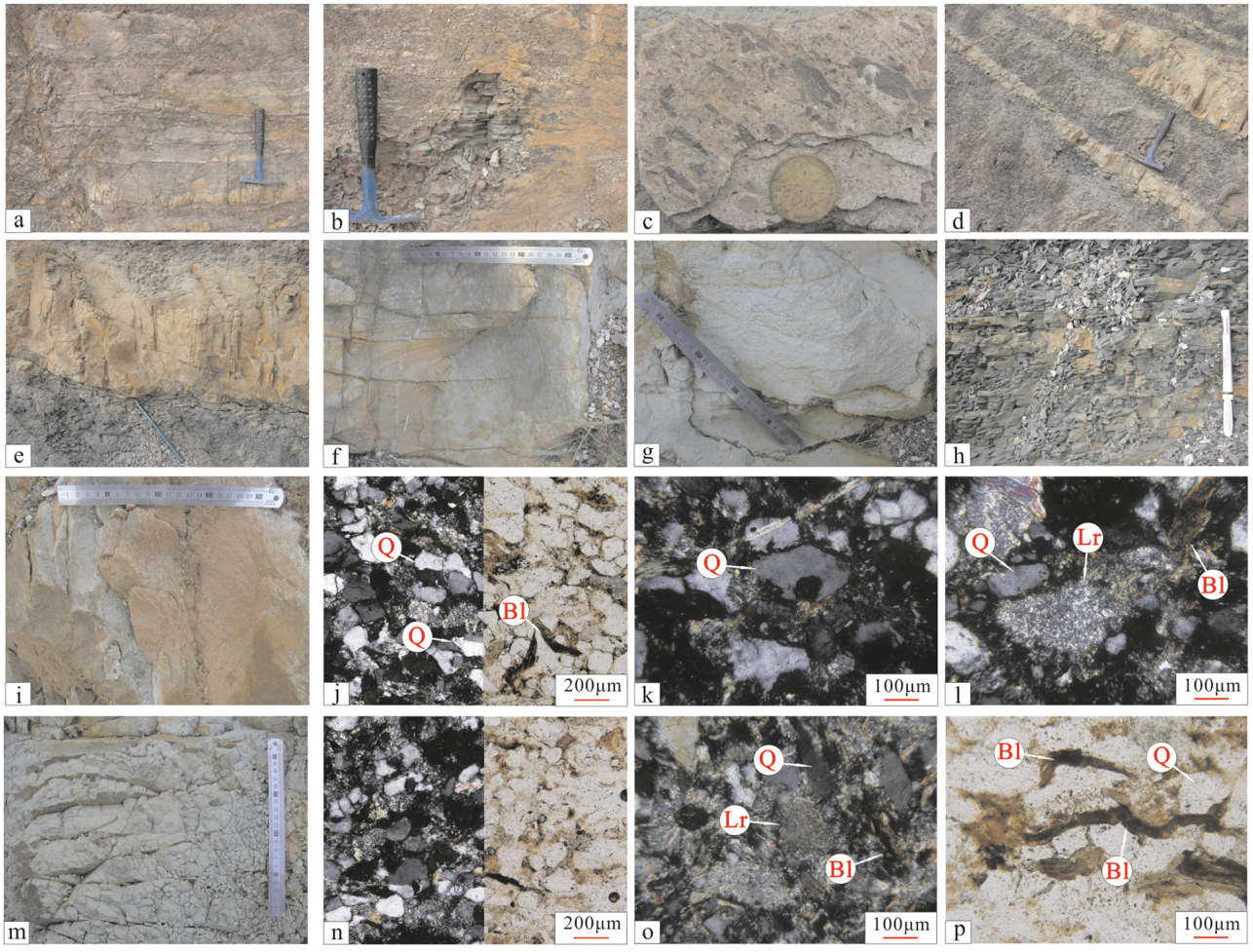

Figure 2: Field photographs and microscopic photographs. (a) The current bedding in the mudstones layers; (b) the horizontal bedding in the mudstones layers; (c) plant fossils and ichthyolites in the silty mudstone layers; (d) the lenticular bedding in the local fine sandstone layers; (e) the erosional surface in the lower part of the fine sandstone layers; (f) the wedge-shaped cross-bedding in the fine sandstone layers; (g) the trough cross-bedding in the fine sandstone layers; (h) the horizontal bedding in the mudstone layers; (i) field photograph of fine grain-size debris quartz sandstone (DK5); (j) fine grain-size clastic texture, the grains are subangular-subrounded, the sort is fair well, the contact relation is concavo–convex contact to line contact; (k) the sample DK5(+), rhyolitic debris; (l) the sample DK5(+), the embayed boundary of quarts; (m) field photograph of fine grain-size debris quartz sandstone (DK15); (n) fine grain-size clastic texture, the grains are subangular-subrounded, the sort is fair well, the primary contact relation is line contact; (o) the sample DK15(+), rhyolitic debris; (p) the sample DK15(+), the blackmica's deformation by the pressure. Q. Quartz; Bl. Blackmica; R. Rhyolitic debris.

The upper Zhangping Formation, which ranges from 1,550 to 2,900 m, is mainly composed of yellow and light purple thick greywacke and conglomeratic sandstone blended with the light gray thin siltstone and mudstone layers. The lower part of the upper Zhangping Formation shows a normal grain sequence sedimentation rhythm, and the upper part of the upper Zhangping Formation shows an inverse grain sequence deposition rhythm. The characteristics of lithology and bedding structures indicate that the upper Zhangping Formation is fan delta facies.

The Zhangping Formation showed a thickening sequence upward, with a reverse grain size order in ascending order (i.e., from small to large) (Figure 1d). The changes in the facies sequence from shallow lacustrine facies to fan delta facies reflect the lowering of the lake level.

Samples used for testing in this study were all collected from lower and middle Zhangping Formation, 17 sandstones among these samples were chosen to perform modal analysis, 12 mudstones were used for elemental geochemical analysis, and two sandstones were used for detrital zircon U–Pb dating. The samples used for the detrital zircon U–Pb dating were collected from the lower part (DK5) and middle part (DK15) of the Zhangping Formation. DK5 and DK15 samples were classified as fine lithic quartz sandstones observed under a microscope.

The DK5 sample was collected in the lower part of the profile. The rock type here is fine lithic quartz sandstone (Figure 2i), and it is fine-grained detrital and massive in structure. The particles are mostly sub-angular to sub-round. The sorting is good, and the contact is bump contact-line contact (Figure 2j). The sample showed particle support and mosaic cementation. The detrital particles mainly consist of 82% quartz, 15% lithic fragments, and 3% feldspar. The particle diameters are concentrated within the range from 0.15 to 0.2 mm. The quartz is mainly the single-crystal quartz type, and the dirty surface can be seen to have a harbor-like dissolution pattern (Figure 2k). The cuttings are mainly volcanic rock detrital (rhyolite and tuff) (Figure 2l), and sericitization occurs often on the surface. The interstitial material is mainly of a miscellaneous type, and the biotite is bent and deformed.

The DK15 sample collected is located in the middle part of the profile. The rock type is fine lithic quartz sandstone (Figure 2m), and it is fine-grained detrital and massive in structure. The particles are mostly sub-angular to sub-round, and the sorting is better. The contact of particles is the line contact type (Figure 2n). The sample showed particle support and mosaic cementation. The detrital particles mainly consist of 80% quartz, 18% lithic fragments and 2% feldspar. The particle diameters are concentrated within the range from 0.15 to 0.2 mm. The quartz surface is dirty. The cuttings are mainly volcanic rock detrital (Figure 2o), and at the same time, bending biotites can be observed (Figure 2p), and the interstitial material is mainly the matrix.

4 Analysis method

4.1 Modal analysis of sandstones

By studying the contents of various components of sandstone samples collected from the known regional tectonic background, Dickinson [37] put forward clastic model triangular diagrams that can reflect the tectonic background of various provenances. There are five triangular diagrams, such as, Q-F-L, Qm-F-Lt, Qp-Lv-Ls, Qm-P-K, and Lm-Lv-Ls. In this paper, we point-counted components of 18 samples, and the main components are monocrystalline quartz (Qm), polycrystalline quartz (Qp), feldspar (F), plagioclase (P), K-feldspar (K), and lithic fragments (L), as well as volcanic (Lv), metamorphic (Lm), and sediment fragments (Ls). A minimum of 400 grains were counted per sample, and a summary of the data is given in Table S1.

4.2 Element geochemical analysis

Twelve mudstones that were fresh and least affected by diagenesis were collected to perform the elemental geochemical analysis. The major element, trace element, and REE analyses were performed at the Beijing Research Institute of Uranium Geology. The major elements were measured by X-ray fluorescence spectrometry, and the analytical precision and accuracy of the major elements were both better than 5%. The trace elements and REEs were measured by inductively coupled plasma mass spectrometry, and the detection limit was less than 0.5 ppm. The detailed instrument parameters and analytical techniques are described by Xu et al. [18]. The final test results represent averages of three times and the results are shown in Table S2.

4.3 Detrital zircons dating

The samples were prepared after pulverization, zircon selection, target preparation, and polishing. The washing, heavy liquid separation, and magnetic separation steps were completed at the rock mineral sorting facilities of the YuNeng Technology Service Co., Ltd, Langfang City, Hebei Province. For the zircon selection, the full account was taken of the color, size, and different crystal forms. In total, 200–250 zircons were selected randomly for target preparation at the Shangpu Co. in Wuhan, Hubei, and these were polished to near the maximum face; then, cathode luminescence (CL) electron imaging was performed. Based on the photographic CL images of zircons and the avoidance of the inclusions and cracks in the zircons when using the transmitted light, the dating ages of the tested zircons were determined.

The zircon U–Pb age determinations were completed at the Northeast Asia Mineral Resources Evaluation of Land and Resources Key Laboratory of Jilin University. The laser ablation work was completed with a COMPExPro type ArF excimer laser (Coherent Company, Germany). The mass spectrometer was a 7,900 type quadrupole plasma mass spectrometry instrument (Agilent, USA). The laser beam spot diameter was 32 μm. The isotope ratio correction was performed by using the standard zircon 91,500 (1,062 Ma) as an external standard. The standard zircon PLE/GJ-1 was used in monitoring as a blind sample. The element content calculations were performed by using the international standard NIST610 as the external standard and Si as the internal standard. Additionally, NIST612 and NIST614 were used in monitoring as a blind sample. The test analysis process was completed following the methods described by Yuan et al. [38]. The calculations for isotope ratios and element contents were performed with Glitter software. The concordant ages and images were processed by using Isoplot/Ex (3.0) [39]. The error given by the analysis data and the zircon U–Pb concordant diagram was 1σ and this reflects the 95% confidence coefficient. The zircon ages that were less than 1,000 Ma were obtained by using the $^{206}Pb/^{238}U$ age values, while the older ones were derived by using a more accurate age of $^{206}Pb/^{207}Pb$ [40,41].

5 Analysis results

5.1 Element geochemical results

Mudstones from the study area have high SiO_2 values in ranges of 56.5–70.7%, high Al_2O_3 contents in ranges of 15.3–22.4%, and low CaO contents in ranges of 0.02–0.09% and ratios of Al_2O_3 to (Na_2O + CaO) ranges from 59 to 101.76. These values and ratios indicate that the main minerals of mudstones from the Zhangping Formation are quartz and feldspar minerals rich in silica and aluminium with a little carbonate. The Primitive mantle-normalized incompatible trace element variation diagrams show that these mudstone samples are in abundances of large-ion lithophile elements the curves of these samples are broadly similar to the curve of upper continental crust (Figure 3), but Sr values of samples are pretty low compared with that of upper continental crust, indicating a dearth of plagioclase. The REE patterns of these samples are all similar to the pattern of the upper continental crust with the

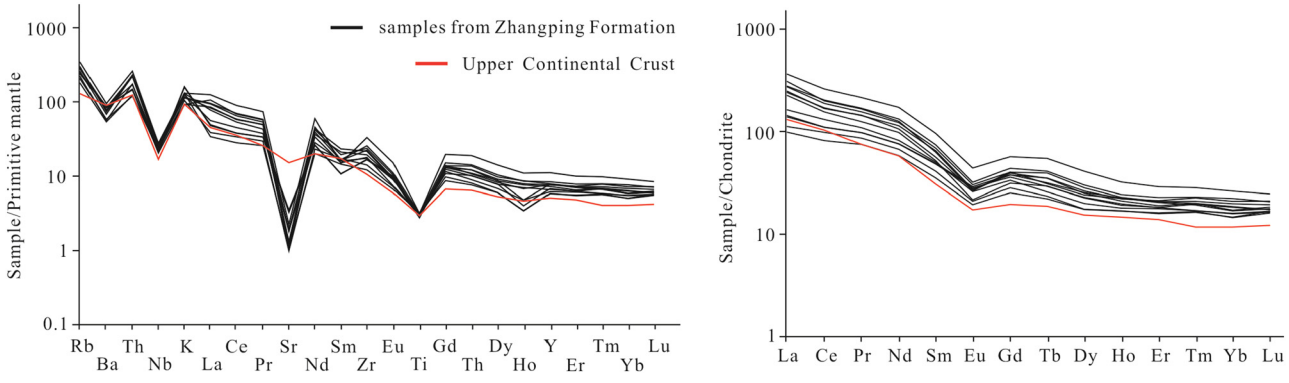

Figure 3: Primitive mantle-normalized spider diagrams and Chondrite-normalized REEs patterns for analyzed samples in the Zhangping Formation. Data for primitive mantle and chondrite are from Sun and McDonough (1989). Data for Upper Continental Crust from (Taylor and Mclennan, 1985).

characteristics of obvious differentiation of light rare earth elements ($(La/Sm)_N$ = 2.7–4.9) and weak differentiation of heavy rare earth element ($(Gd/Yb)_N$ = 1.6–2.2) (Figure 3).

5.2 Zircon U–Pb ages

According to the transillumination and CL images of zircon particles in the DK5 and DK15 samples, particles can be divided into two types, namely, euhedral zircon and well-rounded zircon (Figure 4). The euhedral zircons may represent the near-source zircon approximately, and the well-rounded zircon may represent material that underwent long-distance transport or depositional recirculation. Beside the fact that the individual zircon had a certain core-rim structure, the internal structures were even and the edges showed the development of an oscillating growth zone that was indicative of a magma cause in most of the zircons. A total of 220 U–Pb isotope analyses were conducted on 220 zircon particles randomly selected from the DK5 and DK15 samples (Table S3).

All zircon data were plotted on the U–Pb concordia diagram (Figure 5a and b), but only 209 analyses show a discordance lower than 10%, while those analyses with discordance higher than 10% are marked in red (Figure 5a and b) and were excluded in the element content analyses, isotope ratio analyses, and age statistics. All test points' ages for the two samples range from 180 to 2,662 Ma. DK5 sample results showed one major age peak at ca. 1,848 Ma and two secondary peaks at ca. 235 and 180 Ma (Figure 5c). DK15 sample results showed one major age peak at ca. 1,876 Ma and two secondary peaks at ca. 233 and 190 Ma (Figure 5d). The age compositions of the middle section (DK15) and the lower section (DK5) of the profile were similar.

The contents of Th and U in DK5 and DK15 varied greatly. For DK-5 sample, the Th content ranged from 32.96×10^{-6} to 741.42×10^{-6} and the U content ranged from 73×10^{-6} to 1619.44×10^{-6}. Among the 110 tested points, the Th/U values of most points were greater than 0.1 and the majority of them were greater than 0.4 except for those of DK5-15 and DK5-26, which were 0.09 (Figure 6). For DK-15 sample, the Th contents ranged from 2.58×10^{-6} to 609.04×10^{-6} and the U contents ranged from 57.54×10^{-6} to 1432.31×10^{-6}. Among the 110 tested points, the Th/U values of most points were greater than 0.1 and the majority of them were greater than 0.4, except for the Th/U values of DK15-9, DK15-11, DK15-71, DK15-87, DK15-101, and DK15-104, which were less than 0.1 (Figure 6). The trace and REEs of zircons from DK-5 and DK-15 displayed steep chondrite normalized REE patterns except for DK5-1, DK5-7, DK5-21, DK5-34, DK5-94, DK15-2, DK15-41, DK15-45, DK15-54, DK15-66, and DK15-82 (Figure 5e and f). Combined with the CL images (oscillatory zoning), this indicates that most zircons of the Zhangping Formation are of magmatic origin and a few zircons with ages of ca. 2,000 – 1,800 Ma are of metamorphic origin.

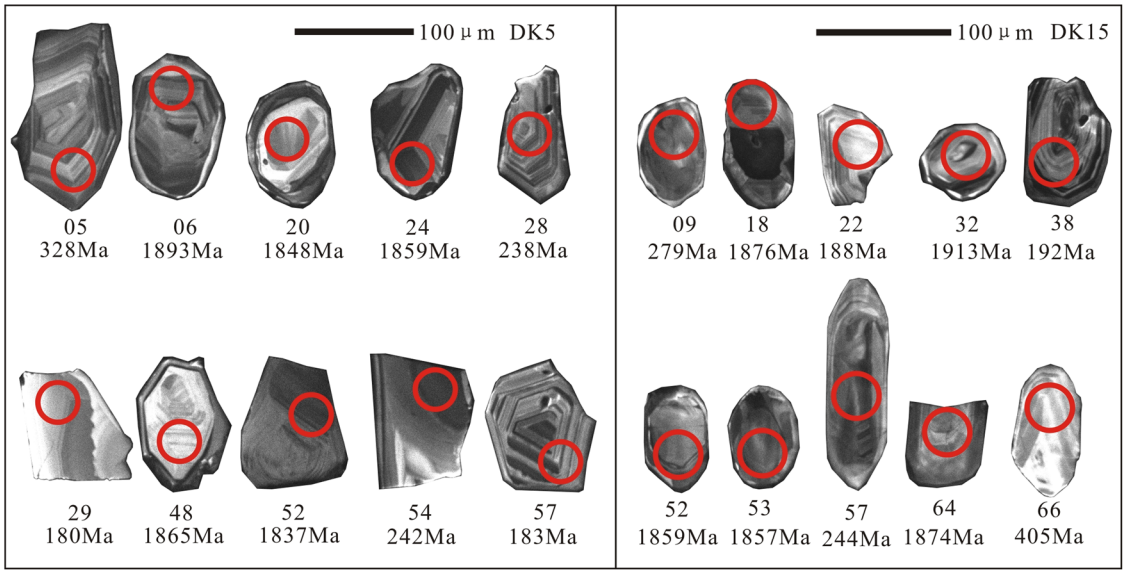

Figure 4: CL images of the zircons and analyzed points. Note: the red circles in the figure are analysis sample points, the values near the zircons are the analysis number and the zircons' age (UI: Ma).

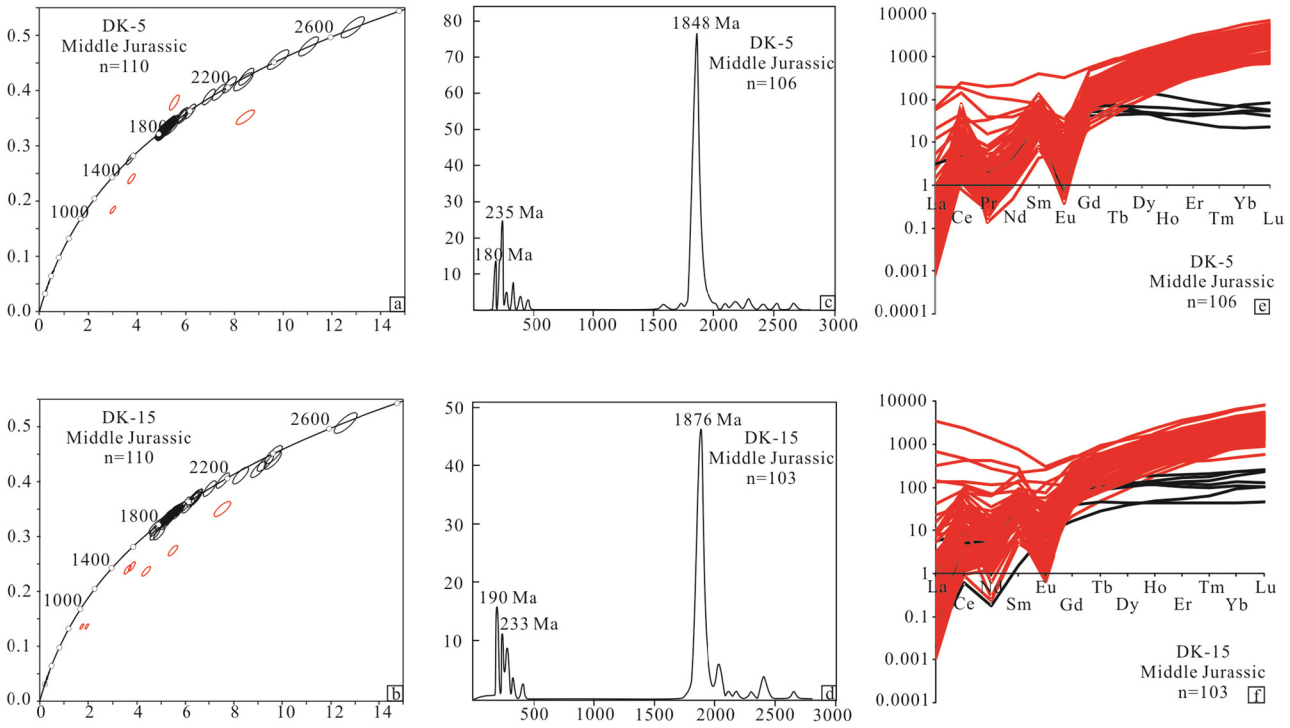

Figure 5: U–Pb concordia diagram, probabilistic histograms, and chondrite-normalized REE patterns of detrital zircons from the analyzed samples of the Middle Jurassic in the southwestern Fujian (chondrite data are from Sun and McDonough (1989)).

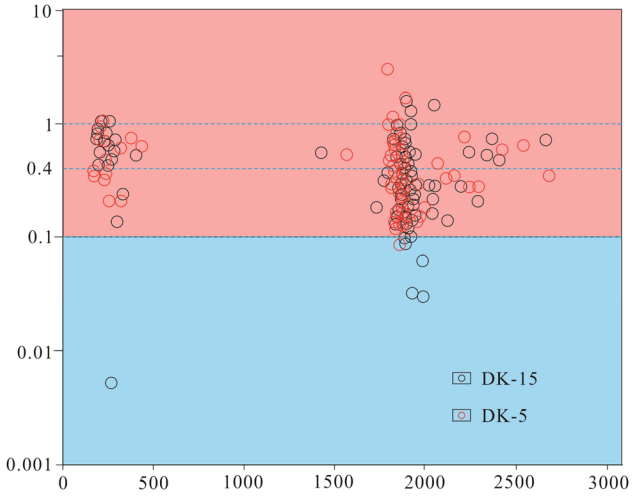

Figure 6: Zircons' ages and Th/U relationship diagram of the Middle Jurassic samples in the Southwestern Fujian.

6 Discussion

6.1 Provenance analysis

6.1.1 Modal analysis

The statistics results were plotted on the Dickinson diagrams (Figure 7). In the QFL diagram, the quartz (Q) content of samples was high, and the point was located in the recycled orogeny area. The positions of sample points of the Zhangping Formation in the QmFLt diagram (where Lt represents total lithic fragments) did not change significantly compared with that in the QFL diagram, and data were just shifted a little downward, indicating that there is no ocean component in the sample. In the QpLvLs diagram, all points of the Zhangping Formation fell into the areas of arc orogen sources and mixed orogenic sands and away from the source area of subduction complex sources and collisional orogen sources. In the QmPK diagram, all samples were located in the land block source area due to the characteristics of high quartz contents and low feldspar contents, indicating that samples have high degree of maturity and stability, while there was a lack of the deep components. In the Lm–Lv–Ls diagram, all samples fell within the area of back-arc, thus indicating that source rocks of the Zhangping Formation are characterized by the tectonic background of the back-arc basin. According to the analysis of the samples' positions in the diagrams, the sedimentary provenance of the Zhangping Formation is mainly from the recycled orogen and the arc orogeny source area.

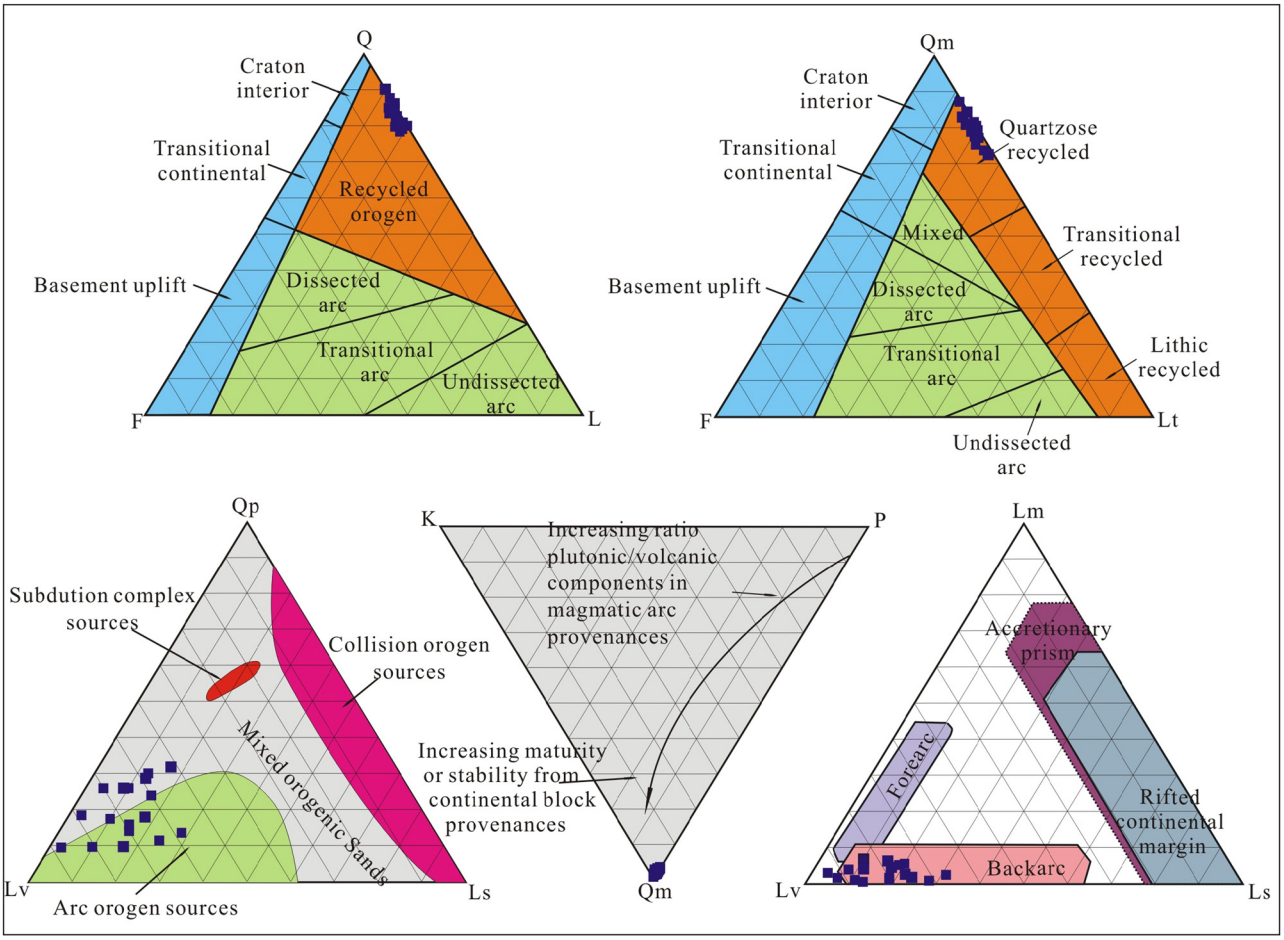

Figure 7: The Dickinson diagrams of the Zhangping Formation sandstones from Southwestern Fujian (the chart is based on the diagram of Dickinson (1985)). Qm, monocrystalline quartz; F, P (plagioclase) + K (potassium feldspar); Lt, total lithic fragments, including Lv (volcanic-rock fragments), Ls (sedimentary-rock fragments), Lm (metamorphic-rock fragments), Qp (polycrystalline quartz, including chert); Qt, total quartz; L, total lithic fragments except polycrystalline quartz (Qp).

6.1.2 Element geochemical analysis

Weathering and other modification effects can influence the major elements in sediments during the process of transport and deposition [42], so it is necessary to distinguish the degree of weathering before the provenance analysis with major elements. The chemical index of alteration (CIA) can indicated weathering degree [43], and the chemical composition variation index (ICV) was used to determine whether clastic sediments were primary deposits or recirculation deposits [44]. ICV-CIA diagram was used to determine the degree of weathering for Zhangping Formation samples, and all samples are plotted within the strong weathering area (Figure 8a), which indicates that the samples in the study area generally experienced strong weathering or recycled deposition. However, some trace and REEs in the mudstone are relatively stable and not affected by weathering and sedimentation, which can well reflect the geochemical properties of the provenance [27]. If the diagenesis causes the loss of trace elements in samples, the Th/Sc and CIA values will show a positive correlation [45]. We analyzed the correlation between Th/Sc and CIA of all samples from Zhangping Formation (Figure 8b). The results show that the correlation coefficient between the Th/Sc and CIA is 0.0363, which indicates that trace elements can well reflect the composition of source rocks. Therefore, the element geochemical test data were plotted on the ∑REE and La/Yb provenance rock discrimination diagrams (Figure 8c), the La/Th–Hf diagram (Figure 8d), the Th–Hf–Co diagram (Figure 8e), and the Th/Sc–Zr/Sc diagram (Figure 8f). In the ∑REE and La/Yb provenance rock discrimination diagram (Figure 8c), most samples fell into the intersection of sedimentary rock and granite except a few samples

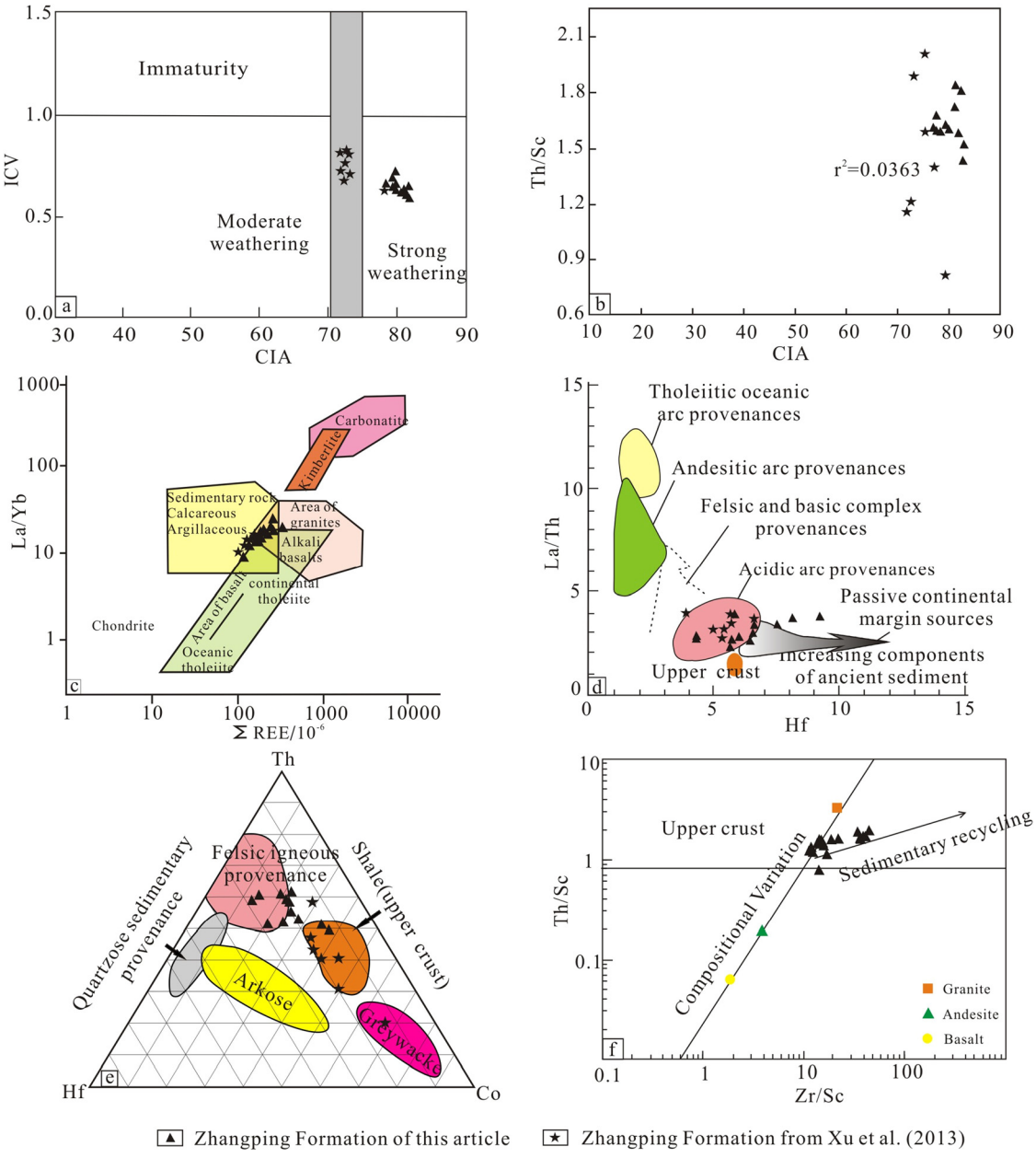

Figure 8: Typical geochemical elements parameters correlation and source material composition discrimination diagram of the Zhangping Formation. (a) CIA-ICV diagram(based on Nesbitt and Young, 1982); (b) CIA-Th/Sc diagram (based on Roddaz et al., 2006); (c) ∑REE-La/Yb diagram (based on Allegre and Minster, 1978); (d) La/Th-Hf diagram (based on Floyd et al., 1989); (e) Th–Hf–Co ternary plot (based on Condie, 1989); (f) Th/Sc–Zr/Sc diagram (based on McLennan et al., 1983).

falling in the granite area and sedimentary rock area. It can be seen that the source rocks of Zhangping Formation are mainly from sedimentary rock and granite. In the La/Th–Hf diagram (Figure 8d), almost all samples are distributed in the acid island arc provenance except two samples falling in the passive continental margin provenance and its vicinity, indicating that the sediments are mainly derived from acid island arc source area and ancient sediments. In the Th–Co–Hf ternary plot (Figure 8e), samples fall in the felsic igneous provenance, shale (upper crust), and greywacke provenance. In the Th/Sc–Zr/Sc diagram (Figure 8f), the samples were mainly distributed along the evolution line of the sedimentary cycle, and all fall within the granite region, indicating that the source rocks of these samples are felsic rocks.

6.1.3 Detrital zircons ages

The high hardness and high closed temperature are key characteristics of zircon, which enable it to maintain a stable U–Pb isotope system after experiencing a variety of geological processes [46,47]. Therefore, using the detrital zircon age spectrum of sediments has become one of the most effective research methods for revealing the source area and making affinity comparisons. In this paper, the detrital zircon ages of sedimentary basins in late Paleozoic-early Mesozoic were applied in comparisons among southwestern Fujian and the East Guangdong basin (southeastern Cathaysia Block), Dongkeng basin of southern Jiangxi and Ji'an basin of middle Jiangxi (middle Cathaysia Block), Hengyang basin of middle-south Hunan and Pingle basin of west Jiangxi (northern Cathaysia Block), Jingdezhen basin of northeastern Jiangxi and Huangshan basin of southwestern Anhui (Yangtze Block), and Jian'ou basin of northern Fujian (eastern Cathaysia Block) (Figures 9 and 10). The results showed that detrital zircon composition of southern South China Block is concentrated in the late Paleozoic-early Mesozoic range, and there is a significant lack in Paleoproterozoic zircons. The zircon age composition of northern South China Block was found to be significantly older than that of southern South China Block, with zircons older than 3,000 Ma. In addition, detrital zircons ages were also compared with typical magmatic rocks from the surrounding potential source area to further determine the source area (Figure 11). The two sets of samples of the Zhangping Formation from the Middle Jurassic in southwestern Fujian were mainly composed of Paleoproterozoic zircon ages and early-Mesozoic zircon ages. From the Mesozoic to Paleoproterozoic, the span of time is very large, and CL images show that older zircons (ca. 1,800 Ma) from the Zhangping Formation are well-rounded, which indicate they are transported and abraded over long distances or were recycled from older strata, while younger zircons (ca. 300–1,900 Ma) are euhedral to subeuhedral, indicating that these zircons may be deposited near source region. The Precambrian detrital zircon ages ranged from 1,948 to 1,801 Ma, and major age peaks were detected at ca. 1,848 and 1,878 Ma. These zircons are mostly subrounded, and a few zircons are rounded, thus indicating that most zircons experienced short transport. Based on

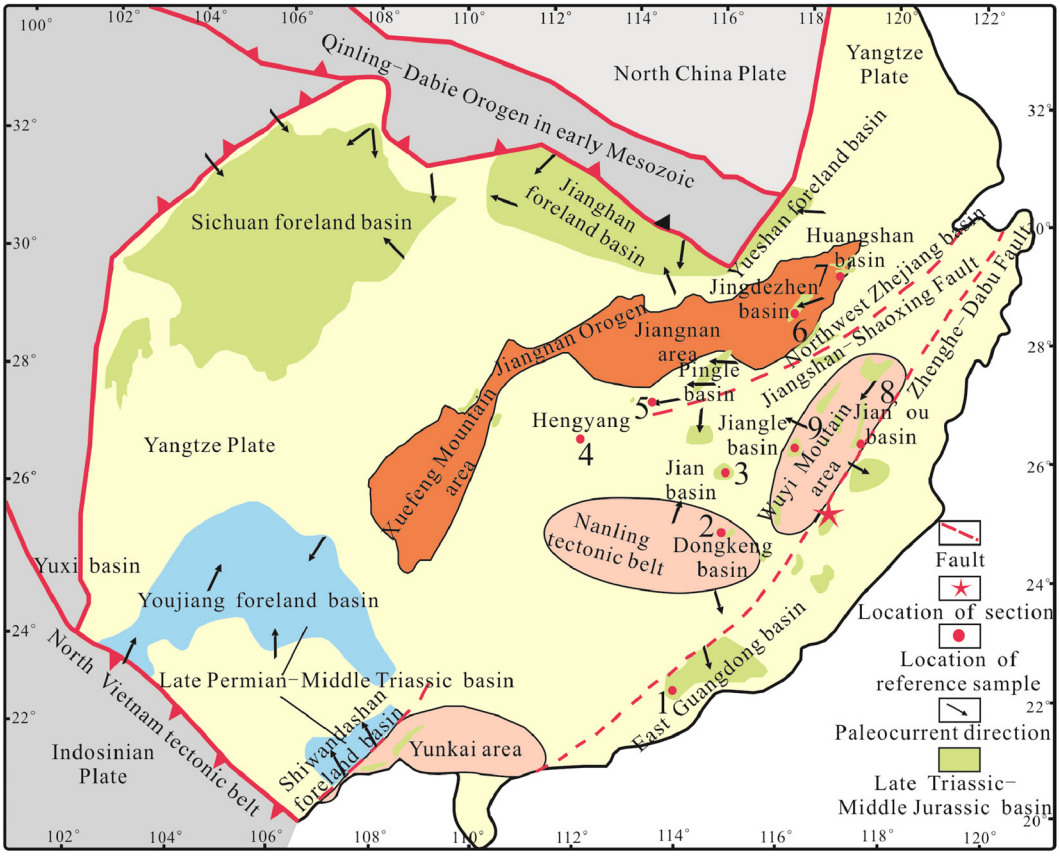

Figure 9: The distribution map of the basins of early Mesozoic in south China Block (after Xu et al. (2016)).

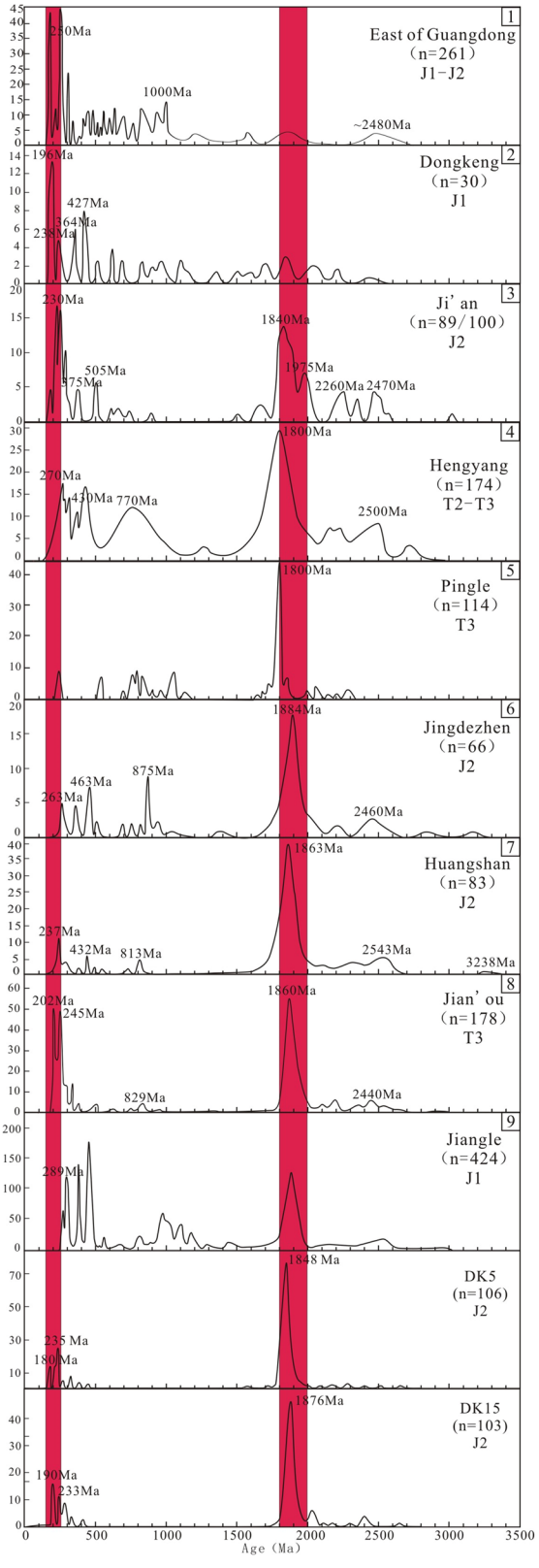

Figure 10: Comparison diagrams of detrital zircon ages in the study area and its surrounding basins. (1) The detrital zircons' age of East Guangdong basin in Early Jurrasic quoted from (Yang and He 2013). (2) The detrital zircons' age of Dongkeng basin in Early Jurrasic quoted from (Li et al. 2013). (3) The detrital zircons' age of Jian basin in Early Jurrasic quoted from (Meng et al. 2015). (4) The detrital zircons' age of Hengyang basin in Middle-Late Triassic quoted from (Yan et al. 2011). (5) The detrital zircons' age of Pingle basin in Upper Triassic quoted from (She 2007). (6) The detrital zircons' age of Jingdezhen basin in Early Jurrasic quoted from (Xu et al. 2016). (7) The detrital zircons' age of Huangshan basin in Early-Middle Jurrasic quoted from (Xu et al. 2016). (8) The detrital zircons' age of Jian'ou basin in Late Triassic quoted from (Yao et al. 2012). (9) The detrital zircons' age of Jiangle basin in Middle Permian quoted from (Li et al. 2012).

the trace element characteristics, most detrital zircons with ages 1,948–1,801 Ma from the study area are magmatic in origin, and a few zircons are metamorphic. Detrital zircons with ages of ca. 1,948–1,801 Ma are widely distributed in the Yangtze Block and Cathaysia Block, whereas there are significant differences. At present, a few granites are reported in the southeastern Yangtze Block aged ca. 1,800 Ma, and most rocks aged at ca. 1,800 Ma are metamorphic rocks [48–51]. There are k-feldspar granites with ages of ca. 1,850 Ma in the Kongling area located in the Yangtze Block [52]; however, the basement still lacks a large number of rock masses of ca. 1,900–ca. 1,800 Ma [53]. In the Cathaysia Block, the granite bodies with ages of 1,900–1,800 Ma are widely distributed in the Wuyi region [54–58]. At the same time, the oldest rocks exposed in the Wuyi region are a set of thick metamorphic rocks, which are part of the Mayuan Group of the Paleoproterozoic [59]. Eastern orogen located in southeastern South China Block began to uplift in the late Paleozoic resulting in a paleocurrent of South China Block in the Late Triassic-Early Jurassic that flowed from north to south, and the paleocurrent direction in the Late Triassic-Early Jurassic was 208° in western Zhejiang and was 215° in western Fujian [60]. Besides, Hengyang, Pingle, Jingdezhen, Huangshan, and Jiangle basins all have major age peaks at ca. 1,800 Ma (Figure 10) [61–64], and these zircons are also derived from Wuyi region.

There exist Indosinian age peaks (ca. 233 and 235 Ma) and Yanshanian age peaks (ca. 180 and 190 Ma) in the early Mesozoic detrital zircons. The early Mesozoic detrital zircons are widely distributed in the Cathaysia Block and Yangtze Block (Figure 11). During the Triassic, the Indochina Block collided with the South China Block [4,5], which led to formation of abundant Indosinian syncollisional granites aged ca. 240 Ma that are widely distributed in northern Guangdong and western Fujian of the Cathaysia Block, such as the Youdong granite bodies with ages of 232 ± 4 Ma of

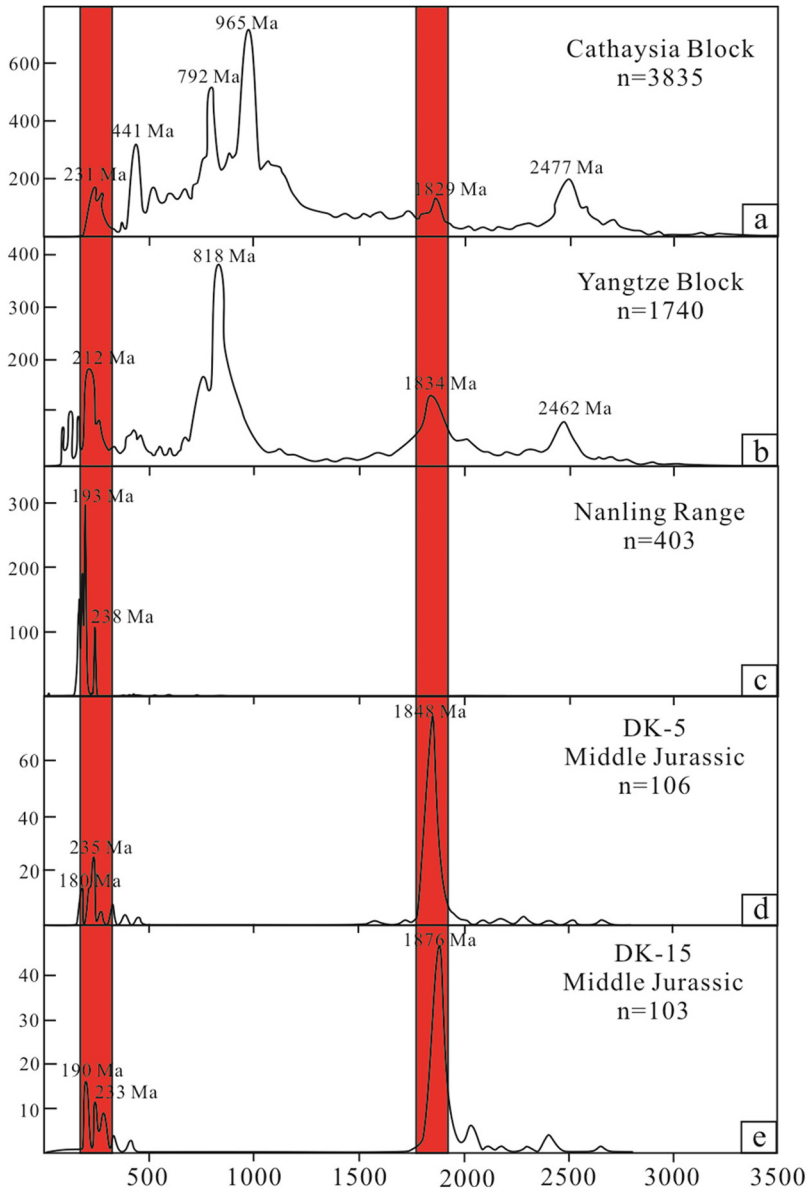

Figure 11: Probability curves of ages for detrital zircons from the southwestern Fujian and the nearby potential source regions. (a) Detrital zircon data of Cathaysia Block from (Xu et al., 2018; Hu et al., 2015; Yang and Jiang, 2018; Xu et al., 2018; Yu et al., 2007, 2008, 2010; Yao et al., 2011; Xu et al., 2007; Wu et al., 2010; Li et al., 2002). (b) Detrital zircon data of Yangtze Block from (Liang et al., 2018; Zhu et al., 2001; Duan et al., 2011; Yan et al., 2011; Wang et al., 2010; Li et al., 2010; Yang et al., 2015). (c) Detrital zircon data of Nanling Range (Ji and Wu, 2010; Xu et al., 2010; Zhu et al., 2010; He et al., 2010). (d, e) Detrital zircon data of this study.

northern Guangdong [65], and the Gutian granite plutons with ages of 235 ± 2.4 Ma of western Fujian [66]. As influenced by the Indosinian movement, Indosinian granites are widely distributed in the Wuyi region, which is located in the western part of the study area. These detrital zircons are euhedral to subhedral, thus indicating that most zircons experienced short-distance transportation. The zircons showed oscillatory zoning and high Th/U ratios, which indicates that the zircons are magmatic in origin. The paleocurrent direction of the southeastern South China Block in the Early-Middle Jurassic was from northeast to southwest [67]. Therefore, the Indosinian granite in the Wuyi area of South China Block may provide the provenance for southwest Fujian.

The Yanshanian detrital zircons of the study area are mostly subangular, with obvious oscillatory zoning, and combined with the trace element characteristics, these findings indicate that most zircons are in origin and experienced short-distance transportation. There exists

evidence of abundant early Yanshanian magmatic activities (200–180 Ma) in the Nanling area (southern Jiangxi, northern Guangdong, and western Fujian) [12,68–70] (Figure 11), such as the Changpu bimodal volcanic rocks with ages of 205–180 Ma in southern Jiangxi [71], the Keshu granites with ages of 194–182 Ma in southern Jiangxi [72], the granodiorites aged ca. 193 Ma and gabbro diabases aged ca. 196 Ma in the Dongkeng basin of southern Jiangxi [73], the Xialan granite bodies with ages of 194 ± 1 Ma, the Wengong granite bodies with ages of 192 ± 1 Ma in northern Guangdong [70], and the Yongding acid volcanic rocks with ages of 188–179 Ma in Fujian [74]. Dongkeng Basin consists of major age peaks at ca. 196 Ma (Figure 9) and its main source area is Nanling Range [3]. Combined with the geochemical characteristics of the Zhangping Formation, granites are the source rocks of the Zhangping Formation. Therefore, the early Yanshanian magmatic rocks in the Nanling area may represent the provenance for southwest Fujian.

6.2 Basin nature in the early-middle Middle Jurassic

The comparison of the tectonic evolution of the global Greenville orogenic belt is one of the most important issues in the research on the reconstruction of supercontinent Rodinia in the Mesoproterozoic. The Greenville orogeny lasted mainly from ca. 1,190 to 980 Ma [75], and the upper limit was ca. 950 Ma [76]. In recent years, many scholars have proposed that the Greenville orogeny in China reflects the Jinning movement induced by the collision of the North China Block and the Yangtze Block [77,78]. Because of the combination and splitting of the Rodinia supercontinent in the late Mesoproterozoic and early Neoproterozoic, and a large number of magmatic rocks and Jinning orogenic belt were developed in the Yangtze Block in these periods [26,79,80]. Wang et al. [26] discovered the presence of ca. 1,190 to 980 Ma detrital zircons in the Wenbinshan Formation of the Late Triassic in southwestern Fujian, thus demonstrating that Greenville rocks provided provenance for southwestern Fujian in the Late Triassic. However, detrital zircons of 980–1,190 Ma only appeared in the upper part of the Wenbinshan Formation and not in the lower part, which may be indicative of the denudation processes of the Jinning orogenic belt. The Indosinian movement formed by the closure of the Paleo-Tethys Ocean and the collision of the Indochina Block and South China Block may have led to the uplift and denudation of the Jinning orogenic belt, which could have provided the detrital zircons with ages of ca. 1,190 to 980 Ma for the upper Wenbinshan Formation. However, detrital zircons with ages of 1,190 to 980 Ma were not found in the Lishan Formation of the Early Jurassic and the Zhangping Formation of the Middle Jurassic, which indicates that the Indosinian movement did not continuously denudate the Jinning orogenic belt. This shows that southwestern Fujian experienced a change in the tectonic regime and the basin nature.

In the Early Jurassic, the Changle–Nanao fault zone located in the southeastern South China Block continues to develop the thrust-nappe structures [34], which controlled the formation and evolution of basins in Guangdong and Fujian regions. Xu et al. [17] analyzed the basin nature of Southwestern Fujian in the Early Jurassic by using sedimentology and element geochemical and proposed that Southwestern Fujian was a compressional basin at that time. However, entering into the Middle Jurassic, the sedimentary facies of Southwestern Fujian changes from delta facies into lacustrine facies; in the late Middle Jurassic, the sedimentary facies changed into delta facies again, and there is a reverse grain size order upward, which reflect

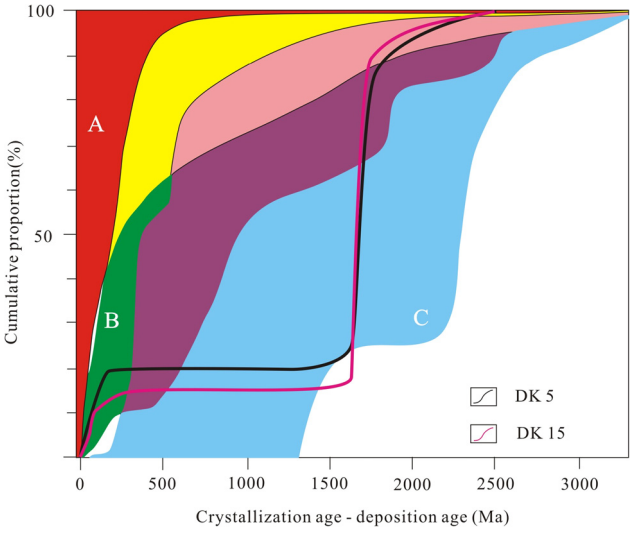

Figure 12: Cumulative proportion curves of variation of the difference between the measured crystallization age for a detrital zircon grain and the depositional age of the Zhangping Formation (modified from Cawood et al. 2012), convergent setting (A, red), collisional setting (B, green), extensional setting (C, blue), transition between convergent-collisional (yellow), transition between convergent-extensional setting (pink), and transition between collisional-extensional setting (purple and pink).

shrinkage of the lake and filling characteristics of basin closure, indicating that southwestern Fujian was controlled by the compressional setting in the late Middle Jurassic. The changes of sedimentary facies show that Southwestern Fujian expanded gradually during the early-middle Middle Jurassic under extensional setting, and began to shrink since the late Middle Jurassic, controlled by compressional setting due to the increased subduction angle of the Paleo-Pacific Block [12]. In recent years, using detrital zircons to determine basin nature has been recognized by many scholars [35,36,81,82]. In the cumulative proportion versus the difference between crystallization age and depositional age diagram proposed by Cawood et al. [81] (Figure 12), two samples of Zhangping Formation all fell into the extensional setting area, which indicate that Southwestern Fujian was extensional basin in the early-middle Middle Jurassic. Moreover, new discriminant diagrams based on major elements and trace elements proposed by Verma and Armstrong-Altrin [32,33] were used to determine the basin nature of Southwestern Fujian in the early Middle Jurassic. Ten samples whose SiO_2 contents were pretty high were chosen to correct their contents and plotted on the discriminant diagrams; the specific discriminant functions were shown by Verma and Armstrong-Altrin [32,33] and Rivera-Gómez et al. [83]. The results show that Southwestern Fujian was rift basin controlled by extensional setting during the early-middle Middle Jurassic (Figure 13). In conclusion, sedimentology, geochemistry, and detrital zircons all suggest that Southwestern Fujian changed from compressional basin of the Early Jurassic into extensional basin of the early-middle Middle Jurassic.

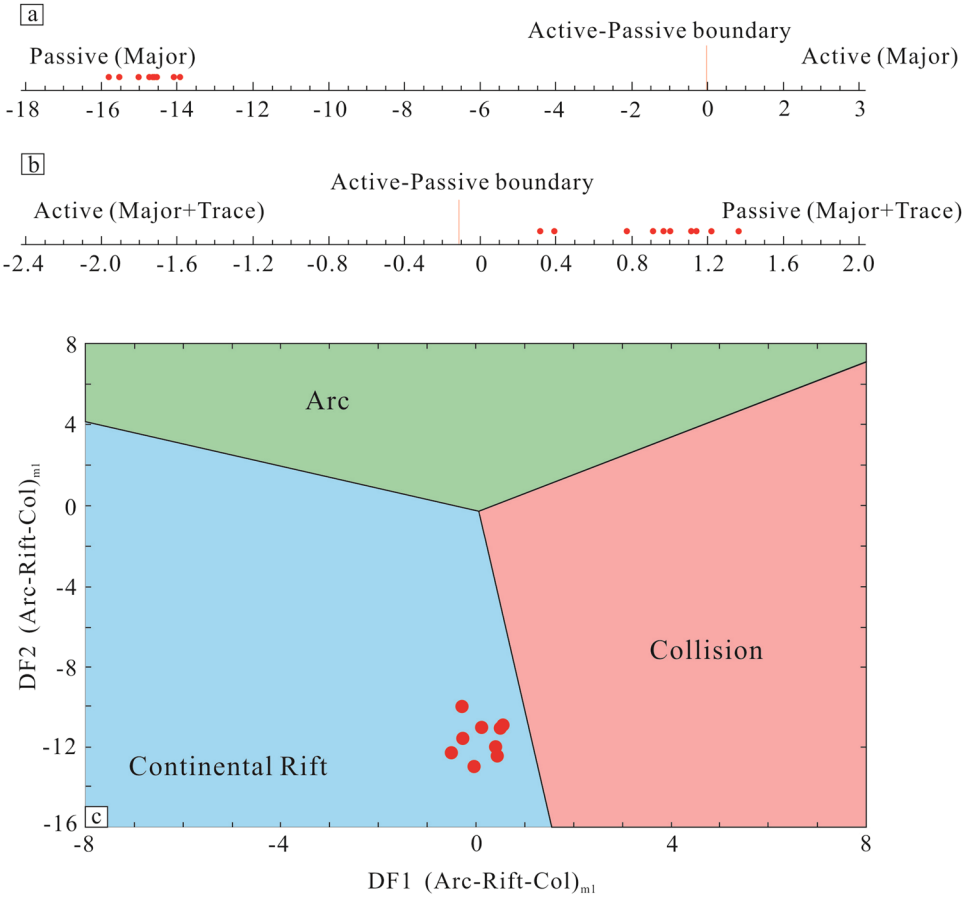

Figure 13: (a) New major element-based multidimensional discriminant function diagram for the discrimination of active and passive margin setting. The specific functions are shown in Verma and Armstrong-Altrin (2016); (b) new combined major and trace element-based multidimensional discriminant function diagram for the discrimination of active and passive margin setting. The specific functions are shown by Verma and Armstrong-Altrin (2016); (c) new discriminant-function multidimensional diagram for high-silica clastic sediments from three tectonic settings (arc, continental rift, and collision).

6.3 Change of tectonic regime in the early Mesozoic

The closure of the Paleo-Tethys Ocean occurred in southwestern South China Block, and the South China and Indochina Blocks collided in the Indosinian period [5,84]. The magmation of South China Block was active from ca. 290 to 260 Ma to ca. 240 to 200 Ma due to the Indosinian movement. During the late stage of the early Jurassic to the Middle Jurassic, the Paleo-Pacific Block subducted beneath the South China Block at a small angle, and this triggered deep mantle activities in the South China Block, thereby changing the deep dynamics of the South China Block. This caused the South China Block enter into the extensional tectonic regime [12,60], and Yanshanian bimodal volcanic rocks were widely distributed [3,85]. The main age peaks of detrital sediments in the East-Guangdong basin changed from ca. 250 to 240 Ma to ca. 180 to 170 Ma, and main sources changed from the Indosinian magmatic rocks located in southern South China Block to the Yanshanian magmatic rocks located in the Nanling region. Yang and He [86] suggested that this change was affected by the volcanic activities in the provenance. The detrital zircon ages of southwestern Fujian in the Late Triassic exhibit age peaks at ca. 220 and 270 Ma [35]. The detrital zircon ages in the Early Jurassic exhibit age peaks at ca. 230 and 280 Ma [35]. The zircon ages of the Zhangping Formation in the Middle Jurassic exhibit relatively obvious age peaks between ca. 240 Ma and ca. 180 to 190 Ma. Although uplift denudation of the erosion area cannot be ruled out, the detrital zircon age peaks of southwestern Fujian in the Late Triassic-Middle Jurassic, which changed from ca. 230 to 220 Ma and ca. 280 to 270 Ma to ca. 180 to 190 Ma, were also affected by the volcanic activity in the source area. The Indosinian magma belt was the major sedimentary source area for southwestern Fujian in the Late Triassic and Early Jurassic [26,35]. Meanwhile, the zircon age peak of ca. 190 to 180 Ma in the sediments of southwestern Fujian in the Middle Jurassic was closely related to the Yanshanian rocks in the Nanling region [13,58,70], indicating that these rocks had replaced Indosinian rocks as the main source rocks in the early-middle Middle Jurassic. These findings indicate that the tectonic regime of southwestern Fujian changed from a Paleo-Tethys tectonic domain in the Late Triassic – Early Jurassic to a Paleo-Pacific tectonic domain in the Middle Jurassic.

7 Conclusion

(1) Element geochemistry results indicate that source rocks of the Zhangping Formation of the Middle Jurassic in Southwestern Fujian are mainly sedimentary rocks and granites; modal analyses results show that the sedimentary provenance of the Zhangping Formation is mainly from the recycled orogen and the arc orogeny source area. The detrital zircon composition of the Zhangping Formation of southwestern Fujian in the Middle Jurassic is mainly composed of Paleoproterozoic (ca. 1,948–1,801 Ma) and early Mesozoic (ca. 235–180 Ma) zircons. The Paleoproterozoic detrital zircons of southwestern Fujian in the Middle Jurassic were mainly from the Wuyi region located in the Cathaysia Block, and a few zircons may have been derived from the Yangtze Block. The late Indosinian zircons may be derived from the Wuyi region, and the Yanshanian zircons may have been derived from the Nanling region.

(2) Sedimentology, geochemistry, and detrital zircons all indicate that Southwestern Fujian changed from compressional basin of the Early Jurassic into extensional basin of the early-middle Middle Jurassic. The major age group changes from ca. 230 to 220 Ma of the Late Triassic – the Early Jurassic to ca. 190–180 Ma of the Middle Jurassic in southwestern Fujian, and the main sources also change from Indosinian granites in the Late Triassic – Early Jurassic to early Yanshanian rocks in the early-middle Middle Jurassic.

Acknowledgments: This work was supported by National Natural Science Foundation of China (41872101; 41402087) and Self-determined Foundation of Key Laboratory of Marine reservoir evolution and hydrocarbon accumulation mechanism, Chinese ministry of education (2019JYB02002).

References

[1] Lu HF. On the cathaysian old land. Geol J China Univ. 2006;12(4):413–7 (in Chinese with English abstract).

[2] Wang GS, Ma WP, Zhu WP. The Late Paleozoic-Early Triassic sedimentary characteristics and its tectonic significance in southwestern Fujian, China. J Chengdu Univ Technol (Sci Technol Ed). 2009;36(1):87–91 (in Chinese with English abstract).

[3] Li WX, Zhao XL, Xing GF, Cen T, Tao J. Geochronology of the detrital zircons from Early Jurassic Sedimentary Rocks from the Dongkeng Basin and its geological implications. Geotecton Metallogen. 2013;37(1):78–86 (in Chinese with English abstract).
[4] Li XH, Li ZX, Li WX, Wang Y. Initiation of the Indosinian Orogeny in South China: evidence for a permian magmatic arc on Hainan Island. J Geol. 2006;114:341–53.
[5] Lepvrier C, Van VN, Maluski H, Truong TP, Tich VV. Indosinian tectonics in Vietnam. Compt Rend Geosci. 2008;340(2–3):94–111.
[6] Wang Y, Fan W, Cawood PA, Ji SC, Peng TP, Chen XY. Indosinian high-strain deformation for the Yunkaidashan tectonic belt, south China: Kinematics and 40Ar/39Ar geochronological constraints. Tectonics. 2007;26(6):TC6008.
[7] Lin W, Wang Q, Chen K. Phanerozoic tectonics of south China block: new insights from the polyphase deformation in the Yunkai massif. Tectonics. 2008;26(6):TC6004.
[8] Liu J, Tran MD, Tang Y, Nguyen QL, Tran TH, Wu WB. Permo-Triassic granitoids in the northern part of the Truong Son belt, NW Vietnam: Geochronology, geochemistry and tectonic implications. Gondwana Res. 2012;22(2):628–44.
[9] Maruyama S, Seno T. Orogeny and relative plate motions: example of the Japanese islands. Tectonophysics. 1986;127:305–29.
[10] Lan CY, Jahn BM, Mertzman SA, Wu TW. Subduction-related granitic rocks of Taiwan. J Southeast Asian Earth Sci. 1996;14(1–2):11–28.
[11] Li XH, Li ZX, Li WX, Wang Y. "Initiation of the Indosinian Orogeny in South China: evidence for a permian magmatic arc on Hainan Island. J Geol. 2006;114:341–53.
[12] Li ZX, Li XH. Formation of the 1300-km-wide intracontinental orogen and postorgenic magmatic province in Mesozoic South China: a flat-slab subduction model. Geology. 2007;35(2):179–82.
[13] He ZY, Xu XS, Niu Y. Petrogenesis and tectonic significance of a Mesozoic granite–syenite–gabbro association from inland South China. Lithos. 2010;119(3–4):621–41.
[14] Cao SH, Tang FL, Huang XS, Qiu WJ, Yuan ZG. Charcteristics and zircon U–Pb geochronology of Metallogenic granitoids in the Gaojiashan Cu–Mo deposits, Northern Wuyishan, Jiangxi Procince. Acta Geol Sin. 2011;85(2):207–12 (in Chinese with English abstract).
[15] Xia KY, Huang CL, Huang ZM. Upper Triassic-Cretaceous sediment distribution and hydrocarbon potential in South China Sea and its adjacent areas. China Offshore Oil Gas. 2004;16(2):74–80 (in Chinese with English abstract).
[16] Zhou D, Sun Z, Chen HZ, Qiu YX. Mesozoic lithofacies, paleogeography, and tectonic evolution of the South China Sea and surrounding areas. Earth Sci Front. 2005;12(3):204–18 (in Chinese with English abstract).
[17] Xu ZJ, Cheng RH, Wang LL, Sheng YJ, Yu ZF. Mineralogical and element geochemical characteristics of the Late Triassic-Middle Jurassic sedimentary rocks in southwestern Fujian Province: Constraints on changes of basin tectonic settings. Acta Petrol Sin. 2013;29(8):2913–24 (in Chinese with English abstract).
[18] Xu ZJ, Cheng RH, Zhang L, Wang LY, Kong Y. Transgression–regression event element geochemistry records of southwestern Fujian in Late Triassic-Middle Jurassic. Journal of Central South University. 2013;20(10):2819–29.
[19] Fedo CM. Detrital zircon analysis of the sedimentary record. Rev Mineral Geochem. 2003;53(1):277–303.
[20] Fonneland, HC, Lien T, Martinsen OJ, Pedersen RB, Kosler J. Detrital zircon ages: a key to understanding the deposition of deep marine sandstones in the Norwegian Sea. Sediment Geol. 2004;164(1–2):147–59.
[21] Link, PK, Fanning CM, Beranke LP. Reliability and longitudinal change of detrital-zircon age spectra in the snake river system, Idaho and Wyoming: an example of reproducing the bumpy barcode. Sediment Geol. 2005;182(1–4):101–42.
[22] Thomas WA. Detrital-zircon geochronology and sedimentary provenance. Lithosphere. 2011;3(4):304–8.
[23] Tapia-Fernandez HJ, Armstrong-Altrin JS, Selvaraj K. Geochemistry and U–Pb geochronology of detrital zircons in the Brujas beach sands, Campeche, Southwestern Gulf of Mexico, Mexico. J South Am Earth Sci. 2017;76:346–61.
[24] Ramos-Vázquez MA, Armstrong-Altrin JS. Sediment chemistry and detrital zircon record in the Bosque and Paseo del Mar coastal areas from the southwestern Gulf of Mexico. Mar Petrol Geol. 2019;110:650–75.
[25] Armstrong-Altrin JS, Ramos-Vázquez MA, Zavala-León AC, Montiel-García PC. Provenance discrimination between Atasta and Alvarado beach sands, western Gulf of Mexico, Mexico: constraints from detrital zircon chemistry and U–Pb geochronology. Geol J. 2018;53(6):2824–48.
[26] Wang, GS, He FB, Zhu WP, Ma WP. U–Pb dating of detrital zircons from late Triassic Wenbinshan Formation in Southwestern Fujian and its geological significance. Geoscience. 2009;23(2):246–56 (in Chinese with English abstract).
[27] McLennan SM, Taylor SR, Kröner A. Geochemical evolution of Archean shales from South Africa. I. The Swaziland and Pongola Supergroups. Precambrian Res. 1983;22(1–2):93–124.
[28] Bhatia MR. Plate tectonics and geochemical composition of sandstones. J Geol. 1983;91(6):611–27.
[29] Armstrong-Altrin JS, Lee YI, Kasper-Zubillaga JJ, Trejo-Ramírez E. Mineralogy and geochemistry of sands along the Manzanillo and El Carrizal beach areas, southern Mexico: implications for palaeoweathering, provenance and tectonic setting. Geol J. 2017;52(4):559–82.
[30] Armstrong-Altrin JS, Botello AV, Villanueva SF, Soto L. Geochemistry of surface sediments from the northwestern Gulf of Mexico: implications for provenance and heavy metal contamination. Geol Quarter. 2019;63(3):522–38.
[31] Anaya-Gregorio, A, Armstrong-Altrin JS, Machain-Castillo ML, Montiel-García PC, Ramos-Vázquez MA. Textural and geochemical characteristics of late Pleistocene to Holocene fine-grained deep-sea sediment cores (GM6 and GM7), recovered from southwestern Gulf of Mexico. J Palaeogeograph. 2018;7(3):253–71.
[32] Verma SP, Armstrong-Altrin JS. New multi-dimensional diagrams for tectonic discrimination of siliciclastic sediments and their application to Precambrian basins. Chem Geol. 2013;355:117–33.

[33] Verma SP, Armstrong-Altrin JS. Geochemical discrimination of siliciclastic sediments from active and passive margin settings. Sediment Geol. 2016;332:1–12.
[34] Li X. Division of tectonic units and basic characteristics of Fujian Province. Global Geol. 2013;32(3):549–57 (in Chinese with English abstract).
[35] Xu, ZJ, Lan YZ, Kong JT, Cheng RH, Wang LL. Detrital zircon U–Pb dating of Late Triassic Wenbinshan Formation in southwestern Fujian, South China, and its geological significance. Canadian J Earth Sci. 2018;55(8):980–96.
[36] Hu LS, Cawood PA, Du Y, Yang J, Jiao L. Late Paleozoic to early Mesozoic provenance record of Paleo-Pacific subduction beneath South China. Tectonics. 2015;34(5):986–1008.
[37] Dickinson WR. Plate tectonics and sedimentation. Soc Econ Paleontog Mineral Spec Publ. 1974;22:1–27.
[38] Yuan HL, Gao S, Liu XM, Li HM, Günther D, Wu FY. Accurate U–Pb age and trace element determinations of zircon by laser ablation inductively coupled plasma mass spectrometry. Geostandards Geoanal Res. 2010;28(3):353–70.
[39] Ludwig KR. User's manual for Isoplot3.0: a geochronological, toolkit for Microsoft Excel Berkeley geochronology center. Special Publication. 2003;4:1–71.
[40] Gehrels, G, Johnsson MJ, Howell DG. Detrital zircon geochronology of the Adams Argillite and Nation River Formation, East entral Alaska. J Sediment Res. 1999;69(1):135–44.
[41] Sircombe KN. Tracing provenance through the isotope ages of littoral and sedimentary detrital zircon, eastern Australia. Sediment Geol. 1999;124:47–67.
[42] Nesbitt HW, Young GM. Early Proterozoic climates and plate motions inferred from major element chemistry of lutites. Nature. 1982;299(5885):715–7.
[43] McLennan SM. Weathering and global denudation. J Geol. 1993;101(3):295–303.
[44] Cox R, Lowe DR, Cullers RL. The influence of sediment recycling and basement composition on evolution of mudrock chemistry in the southwestern United States. Geochim Cosmochim Acta. 1995;59(14):2919–40.
[45] Roddaz M, Viers J, Stéphane B. Controls on weathering and provenance in the Amazonian foreland basin: insights from major and trace element geochemistry of Neogene Amazonian sediments. Chem Geol. 2006;226(1–2):31–65.
[46] Bruguier O, Lancelet JR. U–Pb dating on single detrital zircon grains from the Triassic Songpan-Ganze Flysch (Central China): provenance and tectonic correlations. Earth Planet Sci Lett. 1997;152:217–31.
[47] Xu WL, Wang F, Meng E. Paleozoic-early Mesozoic tectonic evolution in the eastern Heilongjiang Province, NE hina: evidence from igneous rock association and U–Pb geochronology of detrital zircons. J Jilin Univ (Earth Sci Ed). 2012;42(5):1378–89 (in Chinese with English abstract).
[48] Xie GG, Li JH, Li WX, Tang HF, Li HM, Zhou XM. U-Pb zircon dating of Presinian rocks at Lushan MT and its geological implication. Sci Geol Sin. 1997;32(1):110–5.
[49] Ayers JC, Dunkle S, Gao S, Miller CF. Constraints on timing of peak and retrograde metamorphism in the Dabie Shan Ultrahigh-Pressure Metamorphic Belt, east-central China, using U–Th–Pb dating of zircon and monazite. Chem Geol. 2002;186(3–4):315–31.
[50] Li XP, Zheng YF, Wu YB, Chen FK, Gong B, Li YL. Low-T eclogite in the Dabie terrane of China: petrological and isotopic constraints on fluid acticity and radiometric dating. Mineral Petrol. 2004;148(4):443–70.
[51] Yang JS, Wooden JL, Wu CL, Liu FL, Xu ZQ, Shi RD, et al. SHRIMP U–Pb dating of coesite-bearing zircon from the ultrahigh-pressure metamorphic rocks, Sulu terrane, east China. J Metamorph Geol. 2003;21(6):551–60.
[52] Zhao FQ, Zhao WP, Zuo YC, Li ZH. Zircon U–Pb ages of the Migmatites from Kongling complex. Geol Survey Res. 2006;29(2):81–5.
[53] Liu XM, Gao S, Yang JH, Ling WL, Hu ZC, Yuan HL. Precambrian crustal evolution of the Yangtze Craton: U–Pb and Hf-isotope evidence from detrital zircons. Geochim Cosmochim Acta. 2006;70(18):A366.
[54] Wan YS, Liu DY, Xu MH, Zhuang JM, Song B, Shi YR, et al. SHRIMP U–Pb zircon geochronology and geochemistry of metavolcanic and metasedimentary rocks in Northwestern Fujian, Cathaysia block, China: Tectonic implications and the need to redefine lithostratigraphic units. Gondwana Res. 2007;12(1–2):166–83.
[55] Yu, JH, Wang LJ, O'Reilly YS, Griffin WL, Zhang M, et al. A paleoproterozoic orogeny recorded in a long-lived cratonic remnant (Wuyishanterrane), eastern Cathaysia Block. China. Precambrian Res. 2009;174:347–63.
[56] Li, ZX, Li XH, Wartho JA, Clark C, Li WX, et al. Magmatic and metamorphic events during the Early Paleozoic Wuyi-Yunkai Orogeny southeastern South China: new age constraints and P-T conditions. CSA Bull. 2010;122:772–93.
[57] Li XH, Sun M, Wei GJ, Liu Y, Lee CY, Malpas J. Geochemical and Sm–Nd isotopic study of amphibo-lites in the Cathaysia Block, SE China: evidence for extremely depleted mantle in the Paleoproterozoic. Precambrian Res. 2000;102:251–62.
[58] Li, ZX, Li XH, Chuang SL, Lo CH, Xu XS, et al. Magmatic switch-on and switch-off along the South China continental margin since the Permian: transition from an Andean-type to a Western Pacific-type plate boundary. Tectonophysics. 2012;532–535:271–90.
[59] Yu JH, Wei ZY, Wang LJ, Shu LS, Sun T. Cathaysia block: a young continent composed of ancient materials. Geol J China Univ. 2006;12(4):440–7 (in Chinese with English abstract).
[60] Shu LS. An analysis of principal features of tectonic evolution in South China Block. Geol Bull China. 2012;31(7):1035–53 (in Chinese with English abstract).
[61] Xu, XB, Tang S, Lin SF. Detrital provenance of Early Mesozoic basins in the Jiangnan domain, South China: paleogeographic and geodynamic implications. Tectonophysics. 2016;675:141–58.
[62] She ZB. Detrital zireon geochronology of the upper Proterozoie-Mesozoic clastie rocks in the Mid-Upper Yangtze region. China Univ Geosci. 2007:45–120.
[63] Yan Y, Hu XQ, Lin G, Santosh M, Chan LS. Sedimentary provenance of the Hengyang and Mayang basins, SE China, and implications for the Mesozoic topographic change in South China Craton: evidence from detrital zircon geochronology. J Asian Earth Sci. 2011;41(6):494–503.
[64] Li XH, Li ZX, He B, Li WX, Li QL, Gao YY, et al. The Early Permian active continental margin and crustal growth of the Cathaysia Block: Lnsitu U–Pb, Lu–Hf and O isotope analyses of detrital zircons. Chem Geol. 2012;328:195–207.
[65] Huang GL, Cao HJ, Ling HF, Shen WZ, Wang XD, Fu SC. Zircon SHRIMP U–Pb age, geochemistry and genesis of the Youdong

granite in northern Guangdong. Acta Geol Sin. 2012;86(4):577–86 (in Chinese with English abstract).
[66] He WX. Indosinina rock U–Pb zircons age and geological significance in Gutian County of Southwestern Fujian. Geol Fujian. 2015;1:16–25 (in Chinese with English abstract).
[67] Shu LS, Zhou XM, Deng P, Yu XQ. Principal geological features of Nanling Tectonic Belt, South China. Geol Rev. 2006;52(2):251–65 (in Chinese with English abstract).
[68] Chen P, Zhou X, Zhang W, Li HM, Fan CF, Sun T, et al. Petrogenesis and significance of early Yanshanian syenite-granite complex in eastern Nanling Range. Sci China Ser D. 2005;48(7):912–24.
[69] He ZY, Xu XS, Niu Y. Petrogenesis and tectonic significance of a Mesozoic granite–syenite–gabbro association from inland South China. Lithos. 2010;119(3–4):621–41.
[70] Zhu WG, Zhong H, Li DF, He DF, Song XY, Ren T, et al. The Early Jurassic mafic-ultramafic intrusion and A-type granite from northeastern Guangdong, SE China: age, orogin, and tectonic significance. Lithos. 2010;119(3–4):313–29.
[71] Ji CY, Wu JH. The SHRIMP zircon U–Pb dating of felsic volcanic rocks and its geological significance from Yutian Group in Southern Jiangxi. J East China Inst Technol (Nat Sci). 2010;33(2):131–8.
[72] Wang GC. Petrogenesis of Mesozoic intrusive rocks in northwest Fujian and South Jiangxi Province and their geodynamic implications. Diss Nanjing Univ Degree Doctor Sci. 2016:21–65.
[73] Yu JH, O'Reilly SY, Wan L, Griffin WL, Zhou MF, Zhang M, et al. Components and episodic growth of Precambrian crust in the Cathaysia Block, South China: evidence from U–Pb ages and Hf isotopes of zircons in Neoproterozoic sediments. Precambrian Res. 2010;181:97–114.
[74] Xu MH. Early Jurassic Bimodal volcanic rocks and their structure environment in Yongding County, Fujian Province. Geol Fujian. 1992;2:115–25.
[75] Rivers T. Lithotectonic elements of Grenville province: review and tectonic implications. Precambrian Res. 1997;86:117–54.
[76] Fitzsmons ICW. Grenville-age basement provinces in East Antarctica evidence for three seqarate collosional orogens. Geology. 2000;28(10):879–82.
[77] Fan JT. Genetic type and age of the protolith of the Niushan granite gneiss from northern Jiangsu and its geologic significance. Progr Precambrian Res. 2000;23(4):213–20.
[78] Wang MX, Wang CY, Zhao JH. Zircon U/Pb and Hf–O istopes of the Zhouan ultramafic intrusion in the northern margin of the Yangtze Block, SW China: constraints on the nature of mantle source and timing of the supercontinent Rodinia breakup. China Sci Bull. 2012;57(34):3283–94.
[79] Peng SB, Fu JM, Liu YH. The discovery and significance of A-type Charnokite in Southeast Guangxi Province, China. Sci Technol Eng. 2004;4(10):832–4.
[80] Li XH, Li WX, Li ZX, Liu Y. 850–790 Ma bimodal volcanic and intrusive rocks in northern Zhejiang South China: a major episode of continental rift magmatism during the breakup of Rodinia. Lithos. 2008;102(1–2):341–57.
[81] Cawood PA, Hawkesworth CJ, Dhuime B. Detrital zircon record and tectonic setting. Geology. 2012;40(10):875–8.
[82] Xu ZJ, Kong JT, Cheng RH, Wang LL. U–Pb dating of detrital zircons in the eastern Guangdong Basin,South China, and constraints on the tectonic transformation from the Early to Middle Jurassic. Canadian J Earth Sci. 2020;57:477–93.
[83] Rivera-Gómez MA, Armstrong-Altrin JS, Verma SP, Díaz-González L. APMdisc: an online computer program for the geochemical discrimination of siliciclastic sediments from active and passive margins. Turkish J Earth Sci. 2020;29:550–78.
[84] Metcalfe I. Gondwanaland dispersion, Asian accretion and evolution of eastern Tethys. Australian J Earth Sci. 1996;43(6):605–23.
[85] Xie, X, Xu XS, Zou HB, Jiang SY, Zhang M, et al. Large-scale magma effect of the Mesozoic in the southeastern part of China: J2 early basalt. Sci China Ser D. 2005;35(7):587–605 (in Chinese with English abstract).
[86] Yang, ZY, He B. Transform of Jurassic tectonic configuration of South China Block: evidence from U–Pb ages of detrital zircons. Geotecton Metall. 2013;37(4):580–91 (in Chinese with English abstract).